The promotional effect of K on the catalytic activity of Ni/MgAl$_2$O$_4$ for the combined H$_2$O and CO$_2$ reforming of coke oven gas for syngas production

Jin Hyang Lee[*,**], **Kee Young Koo**[*], **Un Ho Jung**[*], **Ji Eun Park**[*,***], **and Wang Lai Yoon**[*,†]

*Hydrogen Laboratory, Korea Institute of Energy Research (KIER), 152 Gajeong-ro, Yuseong-gu, Daejeon 34129, Korea
**Department of Chemical & Biological Engineering, Korea University, 145 Anam-ro, Seongbuk-gu, Seoul 02841, Korea
***Department of Environmental Engineering, Yonsei University, 1 Yonseidae-gil, Wonju, Gangwon-do 26493, Korea

Abstract−A K-promoted 10Ni-(x)K/MgAl$_2$O$_4$ catalyst was investigated for the combined H$_2$O and CO$_2$ reforming (CSCR) of coke oven gas (COG) for syngas production. The 10Ni-(x)K/MgAl$_2$O$_4$ catalyst was prepared by co-impregnation, and the K content was varied from 0 to 5 wt%. The BET, XRD, H$_2$-chemisorption, H$_2$-TPR, and CO$_2$-TPD were performed for determining the physicochemical properties of prepared catalysts. Except under the condition of a K/Ni=0.1 (wt%/wt%), the Ni crystal size and dispersion decreased with increasing K/Ni. The coke resistance of the catalyst was investigated under conditions of CH$_4$: CO$_2$: H$_2$: CO : N$_2$=1 : 1 : 2 : 0.3 : 0.3, 800 °C, 5 atm. The coke formation on the used catalyst was examined by SEM and TG analysis. As compared to the 10Ni/MgAl$_2$O$_4$ catalyst, the K-promoted catalyst exhibited superior activity and coke resistance, attributed to its strong interaction with Ni and support, and the improved CO$_2$ adsorption characteristic. The 10Ni-1K/MgAl$_2$O$_4$ catalyst exhibited optimum activity and coke resistance with only 1 wt% of K.

Keywords: Coke Oven Gas, Combined H$_2$O and CO$_2$ Reforming, Syngas, Coke, Ni-K/MgAl$_2$O$_4$

INTRODUCTION

The implementation of emission trading systems (ETS) and conventions on climate change, such as COP21 (Conference of the Parties), has attracted worldwide attention, and industry-wide efforts are being made toward the reduction of greenhouse gases. The steel industry produces the highest amounts of by-product gases, such as coke oven gas (COG), blast furnace gas (BFG), and Linz-Donawitz converted gas (LDG); also, these gases include greenhouse gases such as CO$_2$ and CH$_4$ [1-3]. Among these gases, COG, which is the by-product gas produced from the manufacture of coke as a reducing agent used for the reduction of iron ore, is composed of H$_2$ (48-55%), CH$_4$ (28-30%), CO (5-7%), N$_2$ (1-3%), and CO$_2$ (2-3%) [4]. COG has been primarily used as a source for heating a blast furnace, and studies have been extensively carried out with the aim of reutilizing by-product gases, waste heat, and CO$_2$ produced during the steelmaking process. Several methods exist for reusing by-product gases, such as the separation of hydrogen by pressure swing adsorption (PSA), as well as methanol synthesis and the production of syngas by reforming [5-8]. For exploiting COG by the value-added utilization of syngas, techniques for utilizing syngas as a reducing agent for manufacturing direct reduced iron (DRI) are being developed; namely, syngas composed of H$_2$ and CO is produced by reforming using CH$_4$ and CO$_2$ contained in COG and CO$_2$ trapped from the blast furnace as reactant. If this syngas is used as a reducing agent for the manufacture of DRI, CO$_2$ emissions during the production of coke will be reduced drastically. Moreover, by using the greenhouse gases CO$_2$ and CH$_4$ as reactants, by-product gases can be recycled, and value-added syngas can be manufactured [9].

Partial oxidation, CO$_2$ reforming, and steam reforming have been primarily investigated as reforming reactions, which produce syngas from COG. However, their range of applications is restricted because of the use of a fixed H$_2$/CO ratio of the produced syngas after each individual reforming reaction [10,11]. As compared to individual reforming, combined H$_2$O and CO$_2$ reforming (CSCR), in which reforming occurs by competition between steam and CO$_2$, allows for the regulation of the ratio of the produced H$_2$/CO by varying the feed ratios of H$_2$O and CO$_2$ as reactants [12,13]. The CSCR of methane involves the following reactions [14]:

Steam reforming (CH$_4$+H$_2$O↔3H$_2$+CO, $\Delta H^o_{298\,K}$=206 kJ/mol)
CO$_2$ reforming (CH$_4$+CO$_2$↔2H$_2$+2CO, $\Delta H^o_{298\,K}$=247 kJ/mol)
Water-gas shift reaction (H$_2$O+CO↔H$_2$+CO$_2$, $\Delta H^o_{298\,K}$=−41 kJ/mol)

Moreover, in large-scale commercial reforming, as compared to expensive precious metal catalysts, Ni-based catalysts have been extensively used, attributed to their good activity and cost-effectiveness. However, Ni-based catalysts are easily deactivated by the deposition of coke and the sintering of the catalyst at high temperatures, as well as by sulfur poisoning [15-17]. Hence, several studies have been conducted by the addition of basic alkali metals as promoters; with the addition of alkali metals as promoters, the basicity of the catalyst is enhanced, which in turn increases the adsorption of CO$_2$; increased amounts of adsorbed CO$_2$ inhibit the deposition of carbon via the promotion of the gasification of the deposited coke [1,18]. Frusteri et al. [19] conducted CO$_2$ reform-

ing using a K-promoted Ni/MgO catalyst and showed that the Boudouard reaction, which results in the deposition of carbon, is inhibited, and sintering resistance is improved because of the promotion by K. Luna et al. [20] investigated the activity and coke resistance of catalysts, which were prepared by the addition of 0.5 wt% of K, Sn, Mn, and Ca into $Ni-Al_2O_3$ catalysts via the sol-gel method during CO_2 reforming, and observed that the K-promoted $Ni-Al_2O_3$ catalyst, as compared to $Ni-Al_2O_3$ catalyst without K, exhibits stable catalytic activity, attributed to the strong metal-to-support interaction (SMSI) between Ni and the support, as well as decreased coke deposition. Juan et al. [21] reported that with the addition of the promoter K into a $Ni/\gamma-Al_2O_3$ catalyst, the reduction temperature of the catalyst increases as K enhances SMSI. The lowest coke deposition and highest activity in CO_2 reforming are observed with the addition of 0.2 wt% of K. Hu et al. [22] investigated the steam reforming of acetic acid with the addition of various promoters (such as Li, Na, K, Mg, Fe, Co, Zn, Zr, La, and Ce) into a Ni/Al_2O_3 catalyst. They found that K-promotion increases the number of Ni active sites and inhibits the deposition of coke via the promotion of coke gasification. Hence, K-promoted Ni/Al_2O_3 catalysts demonstrate higher stability and better activity as compared to those without K. Another study reported that the addition of K prevents the deposition of coke by the decomposition of CH_4 in steam reforming, attributed to the decrease of the acid site concentration of the support, as well as improves the activity of a Ni-La-K/cordierite catalyst [23].

In this study, K, serving as a promoter, was added into the $Ni/MgAl_2O_4$ catalyst for improving its catalytic activity and coke resistance in the CSCR of COG. The effects of the variation of K concentration on the basicity and coke resistance of the catalyst were investigated for determining the optimal amount of K required for promotion. In addition, the changes in the H_2/CO ratio of the produced syngas were investigated by varying the H_2O/CO_2 in the CSCR of COG.

EXPERIMENTAL

1. Catalyst Preparation

$Ni(NO_3)_2 \cdot 6H_2O$ (Junsei) and KNO_3 (Junsei) were used as precursors for Ni and K, respectively, and the $10Ni-(x)K/MgAl_2O_4$ catalyst was prepared by co-impregnation. The $MgO-Al_2O_3$ (MgO= 30 wt%, Sasol) support was prepared by calcination at 800 °C for 6 h under air. The Ni content was maintained constant at 10 wt%, while the K concentration was varied (0, 1, 2.5, and 5 wt%). The catalyst was calcined at 800 °C for 6 h under air after loading with Ni and K.

2. Characterization

X-ray diffraction (XRD, D/Max-2500pc, Rigaku Co.) was performed for confirming the compositional homogeneity and catalyst structure of the prepared catalyst. The crystal size of the reduced Ni catalyst, prepared by heating the catalyst at 900 °C for 1.5 h under H_2, was calculated by the Scherrer equation. The specific surface area of the catalyst was measured using a Belsorp-max system (BEL Japan Inc.). For this purpose, 0.2 g of sample was pretreated at 300 °C under vacuum, and the physical adsorption of nitrogen was measured using liquid nitrogen at −197 °C. The dispersion

and surface area of Ni, an active metal in the catalyst, were measured using a BEL METAL-3 system (BEL Japan Inc.). 50 mg of sample was reduced at 900 °C for 1.5 h under H_2, followed by purging at 900 °C for 50 min under Ar. H_2-chemisorption was conducted by injecting a gas pulse of 20% H_2/Ar after cooling the sample to 50 °C. The amount of adsorbed H_2 was estimated under the assumption of one H atom per Ni surface atom ($H/Ni_{surface}=1$). The reduction temperature, as well as the reducibility of the prepared catalyst, was examined by H_2-temperature programed reduction (H_2-TPR) analysis (BEL CAT B, BEL Japan Inc.). 0.1 g of sample was pretreated at 30 °C for 30 min under Ar, and measurements were conducted with increasing temperature from 30 °C to 1,000 °C at a heating rate of 10 °C/min under 10% H_2/Ar. CO_2-TPD (AutoChem 2920, Micromeritics, USA) analysis was performed for determining the basicity of the catalyst; for this purpose, 50 mg of sample was placed in a U-shaped quartz reactor and pretreated at 900 °C for 1.5 h under 10% H_2/Ar. The sample was then cooled to 50 °C, and CO_2 was adsorbed for 1 h under a gas flow of 10% CO_2/He. CO_2 weakly adsorbed on the catalyst surface were removed by purging with He. The sample was heated from 50 °C to 900 °C at a heating rate of 10 °C/min under He, and desorbed CO_2 was detected using a thermal conductivity detector (TCD). The amount of desorbed CO_2 was obtained by performing integral calculus on the CO_2-TPD curve. After the reaction, the formation of coke was observed by SEM (HITACHI, S-4800), and the amount of coke deposited on the surface of the used catalysts was examined by thermogravimetric (TG) analysis (TGA/SDTA 8513, Mettler Toledo). TG analysis was performed by heating 70-90 mg of samples from 50 °C to 800 °C at a heating rate of 5 °C/min under air.

3. Catalytic Reaction

The catalyst thus prepared, with a size of 60-100 mesh, and diluent $MgAl_2O_4$ were mixed and charged in a fixed-bed 3/8″ quartz reactor, and the catalyst performance was tested for the CSCR of COG. Prior to tests, the catalyst was reduced under 50% H_2/N_2 at 900 °C for 1.5 h at 5 atm. Simulated COG was composed of 27% CH_4, 3% CO_2, 55% H_2, 8% CO, and 5% N_2. The reactant feed ratio was $CH_4:H_2O:CO_2:H_2:CO:N_2=1:0.4-1.2:0.4-1.2:2:0.3:0.3$, and the gas mixture was fed into the reactor at a gas hourly space velocity (GHSV) of 4,680 L/h·g_{cat}. CSCR was performed at 900 °C under 5 atm, and the H_2/CO-ratio of the syngas thus produced was investigated by regulating the reactant (CO_2 and H_2O) feed ratio. For the facile formation of coke, it was examined in the absence of H_2O at 800 °C for greater than 50 h at 5 atm under harsh conditions. A feed ratio of $CH_4:CO_2:H_2:CO:N_2=1:1:2:0.3:0.3$ and a GHSV of 500 L/h·g_{cat} were utilized in the reaction. After the condensation and removal of residual water in the effluent by passing it through a trap, gas composition was analyzed by micro-gas chromatography (GC, Agilent 3000). The thermodynamic equilibrium value was calculated using HSC chemistry® 7.1 software.

RESULTS AND DISCUSSION

1. Catalyst Characterization

Fig. 1 shows the results obtained from XRD analysis after the reduction of the $10Ni-(x)K/ MgAl_2O_4$ catalysts, which were prepared with different K contents. Only $MgAl_2O_4$ and Ni peaks were
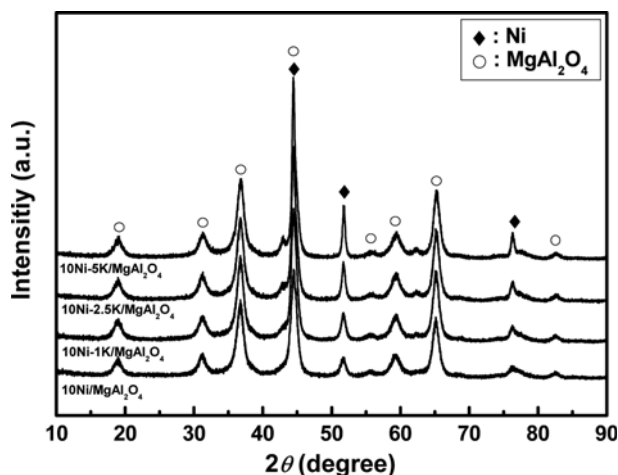
Fig. 1. XRD patterns of reduced 10Ni-(x)K/MgAl$_2$O$_4$ catalysts (K= 0-5 wt%).

Fig. 2. H$_2$-TPR patterns of 10Ni-(x)K/MgAl$_2$O$_4$ catalysts (K=0-5 wt%).

observed, while characteristic peaks corresponding to K$_2$O were not observed. For the 10Ni-5K/MgAl$_2$O$_4$ catalysts, the characteristic peaks of K$_2$O were also not observed, attributed to the highly dispersed K on the support surface. This observation was in agreement with that reported previously by Iwasa et al. [24], who reported that for Ni catalysts containing excess 10 wt% K, characteristic peaks of K were not observed, attributed to highly dispersed K on the support surface. Characteristic peaks for Ni were observed at 2θ=44.3^o, 51.7^o, and 76.2^o, and the Ni crystal size was calculated using the peak observed at 2θ=51.7^o. The crystal size of Ni in the 10Ni/MgAl$_2$O$_4$ catalyst was 9.1 nm, which increased to 12.2-23.2 nm by the addition of K.

Table 1 summarizes the physicochemical properties of the prepared catalysts, such as the BET specific surface area, Ni crystal size, Ni dispersion, Ni surface area, as well as the amount of desorbed CO$_2$. From the measurements of Ni dispersion and Ni surface area by H$_2$-chemisorption analysis, the 10Ni/MgAl$_2$O$_4$ and 10Ni-1K/MgAl$_2$O$_4$ catalysts exhibited similar values of 3.1% and 2.1 m^2/g and 3.0% and 2.0 m^2/g, respectively. However, the catalyst promoted with greater than 2.5 wt% K exhibited decreased Ni dispersion and Ni surface areas of 1.2-1.7% and 0.8-1.2 m^2/g, respectively. Promotion by K greater than a specific amount (K>2.5 wt%) was observed to result in an increased Ni crystal size, as well as decreased
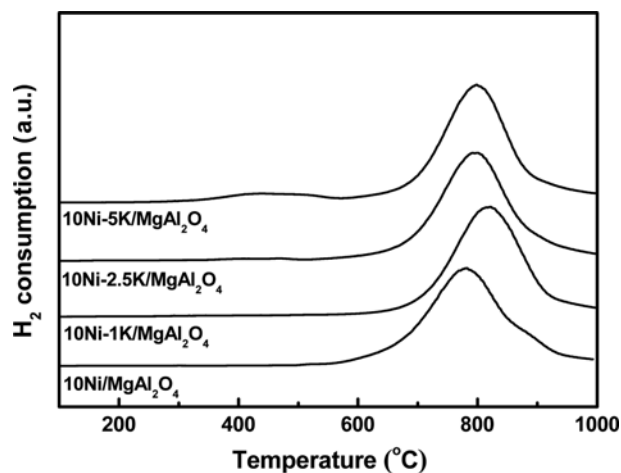
Ni dispersion, and adverse effects on the catalyst characteristics.

Fig. 2 shows the results obtained from the H$_2$-TPR analysis of the prepared 10Ni-(x)K/MgAl$_2$O$_4$ catalysts. The peak observed at around 800 ^{o}C corresponded to the reduction of complex NiO species, corresponding to strong interaction between Ni and MgAl$_2$O$_4$ support [18]. For the 10Ni/MgAl$_2$O$_4$ catalyst without K, the highest reduction peak was observed at 780 ^{o}C, while the reduction peaks of the K-promoted catalysts were observed at higher temperatures. The 10Ni-1K/MgAl$_2$O$_4$ catalyst exhibited the highest reduction peak at 821 ^{o}C. Previously, the reduction peaks of catalysts with alkali metals added as promoters were reported to shift to high temperatures, as SMSI was enhanced, and these catalysts exhibited stable activity for the CSCR of methane [12,13]. Hence, it is expected that the K-promoted 10Ni-(x)K/MgAl$_2$O$_4$ catalyst, exhibiting a reduction peak at a high temperature caused by SMSI enhancement, is more stable than 10Ni/MgAl$_2$O$_4$ for the CSCR of COG.

CO$_2$-TPD analysis was performed for determining the basicity of the prepared catalysts. Table 1 summarizes the amounts of desorbed CO$_2$. The amount of the desorbed CO$_2$ for the K-promoted 10Ni-(x)K/MgAl$_2$O$_4$ catalysts ranged between 0.615 and 0.653 mmol/ g; these values are greater than that of desorbed CO$_2$ obtained for the 10Ni/MgAl$_2$O$_4$ catalyst (0.202 mmol/g). These results indicate that the promotion by K results in the increase of adsorbed CO$_2$.

Table 1. Characteristics of 10Ni-(x)K/MgAl$_2$O$_4$ catalysts prepared with various K/Ni ratios

K/Ni ratio (wt%/wt%)	BET surface area (m^2/g)[a]	Ni crystal size (nm)[b]	Ni dispersion (%)[c]	Ni surface area (m^2/g)[c]	Total desorbed CO$_2$ (mmol/g)[d]
0.0	90.5	9.1	3.1	2.1	0.202
0.1	90.8	12.2	3.0	2.0	0.653
0.25	93.9	16.8	1.7	1.2	0.640
0.50	91.9	23.2	1.2	0.8	0.615

[a]Estimated from N$_2$ adsorption at −196 ^{o}C

[b]Estimated from XRD

[c]Estimated from H$_2$-chemisorption at 50 ^{o}C

[d]Estimated from the integration of CO$_2$-TPD peaks

As mentioned previously, basic catalysts promote coke gasification, attributed to increase in CO_2 adsorption, which in turn stabilizes catalytic activity by inhibiting the deposition of coke. In this study, more facile removal of coke is expected because the increased amount of adsorbed CO_2 caused by K-promotion will promote coke gasification.

Table 2. Reaction results over K-promoted 10Ni/MgAl$_2$O$_4$ catalysts at 900 °C in CSCR of COG (Reaction conditions: CH$_4$:H$_2$O: CO$_2$:H$_2$:CO:N$_2$=1:1.2:0.4:2:0.3:0.3, GHSV=4,680 L/h· g$_{cat}$, 5 atm)

K/Ni ratio (wt%/wt%)	CH$_4$ conversion (%)	CO$_2$ conversion (%)	H$_2$/CO ratio
0.0	79.4	50.4	3.18
0.10	85.5	61.5	3.17
0.25	84.6	57.4	3.26
0.50	83.3	58.0	2.92
Thermodynamic equilibrium	91.3	65.9	3.03
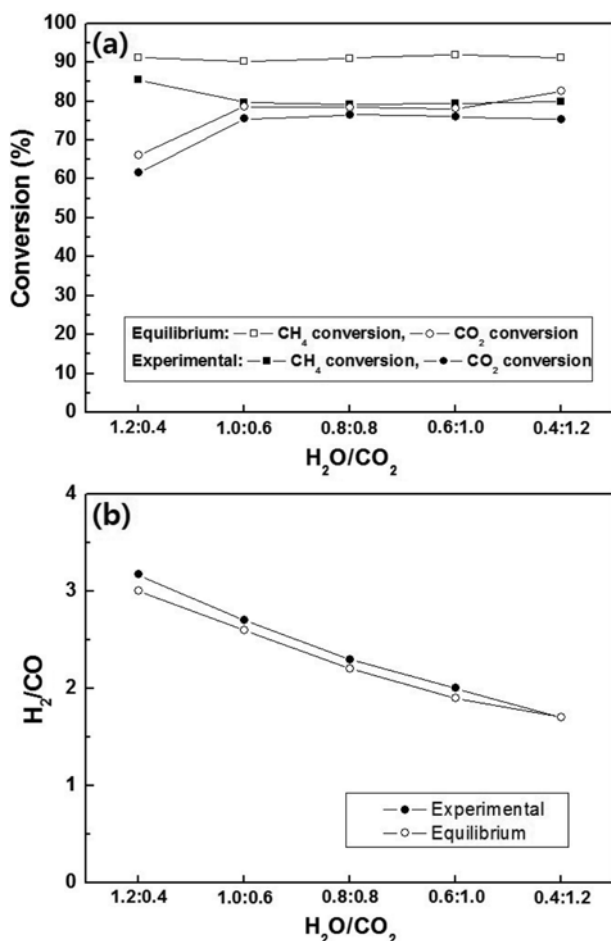
Fig. 3. Effect of H$_2$O/CO$_2$ feed ratio on (a) CH$_4$ and CO$_2$ conversions and (b) H$_2$/CO ratio of 10Ni-1K/MgAl$_2$O$_4$ catalyst in CSCR of COG (reaction conditions: CH$_4$:H$_2$O:CO$_2$:H$_2$:CO:N$_2$= 1:0.4-1.2:0.4-1.2:2:0.3:0.3, 900 °C, 5 atm, GHSV=4,680 L/ h·g$_{cat}$).

2. Activity of Ni-(x)K/MgAl$_2$O$_4$ Catalyst for the CSCR of COG

Table 2 summarizes the results obtained from the CSCR of COG using 10Ni-(x)K/MgAl$_2$O$_4$ catalysts prepared with different K/Ni ratios. CSCR was performed at 900 °C and 5 atm with a GHSV of 4,680 L/h·g$_{cat}$ and a feed ratio of CH$_4$:H$_2$O:CO$_2$:H$_2$:CO:N$_2$= 1:1.2:0.4:2:0.3:0.3. For the 10Ni-(x)K/MgAl$_2$O$_4$ catalysts, the CH$_4$ and CO$_2$ conversion was greater than that for the 10Ni/MgAl$_2$O$_4$ catalyst. The 10Ni-1K/MgAl$_2$O$_4$ catalyst exhibited the highest CH$_4$ and CO$_2$ conversion of 85.5% and 61.5%, respectively. With the addition of marginal amounts of K, the initial catalytic activity improves, and less catalyst deactivation is observed. The decreased catalytic activity with increasing K content was closely related to the catalyst characteristics, as the dispersion and surface area of Ni decreased with increasing K content. For the 10Ni-(x)K/MgAl$_2$O$_4$ catalyst, the CO$_2$ conversion was greater than that of the 10Ni/ MgAl$_2$O$_4$ catalyst as the promotion of K contributed to the increased amount of adsorbed CO$_2$. This result is in agreement with the amounts of desorbed CO$_2$ shown in Table 1. The 10Ni-1K/MgAl$_2$O$_4$ catalyst, which exhibited the highest desorbed CO$_2$ of 0.653 mmol/ g, exhibited the highest CO$_2$ conversion of 61.5%.

Hence, the 10Ni-1K/MgAl$_2$O$_4$ catalyst, which exhibited the highest conversion for both CH$_4$ and CO$_2$, was used for investigating the effects of different H$_2$O/CO$_2$ feed ratios on CH$_4$ and CO$_2$ conversion and H$_2$/CO ratio in the CSCR of COG (Fig. 3). The reaction was performed at 900 °C and 5 atm with a GHSV of 4,680 L/h· g$_{cat}$. By varying the H$_2$O/CO$_2$ feed ratios, the thermodynamic equilibrium values for CH$_4$ conversion exhibited no significant differences. With the exception of H$_2$O:CO$_2$=1.2:0.4, similar CH$_4$ conversion was observed, regardless of the variation in the H$_2$O/CO$_2$ feed ratios. With the addition of K, the resulting experimental values for CO$_2$ conversion were similar to the thermodynamic equilibrium value, caused by the increased amount of adsorbed CO$_2$ [12]. Furthermore, syngas with a H$_2$/CO ratio of 1.7-3.1 could be produced by regulating the H$_2$O/CO$_2$ feed ratio. Thus, the H$_2$O/CO$_2$ feed ratio in CSCR of COG can be regulated for producing the desired H$_2$/ CO ratio.
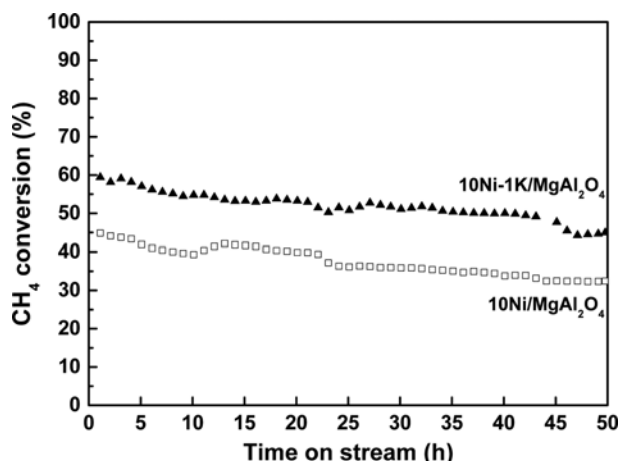

Fig. 4. CH$_4$ conversion with time on stream (TOS) over 10Ni/ MgAl$_2$O$_4$ and 10Ni-1K/MgAl$_2$O$_4$ catalysts in CO$_2$ reforming of COG (Reaction conditions: CH$_4$:CO$_2$:H$_2$:CO:N$_2$=1:1:2: 0.3:0.3, GHSV=500 L/h·g$_{cat}$, 800 °C, 5 atm).
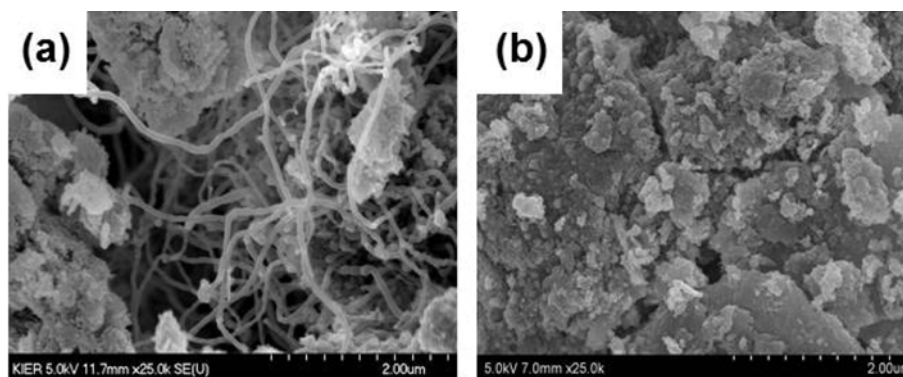
Fig. 5. SEM images of used (a) 10Ni/MgAl$_2$O$_4$ and (b) 10Ni-1K/MgAl$_2$O$_4$ catalysts (Reaction conditions: CH$_4$: CO$_2$: H$_2$: CO : N$_2$=1 : 1 : 2 : 0.3 : 0.3, GHSV=500 L/h·g$_{cat}$, 800 ^{o}C, 5 atm, TOS=50 h).

3. Investigation of Coke

For investigating the promotion effects of K on carbon deposition, CO$_2$ reforming was conducted using the 10Ni/MgAl$_2$O$_4$ and 10Ni-1K/MgAl$_2$O$_4$ catalysts in the absence of H$_2$O (Fig. 4). The reaction was conducted at 800 ^{o}C and 5 atm for 50 h with a feed ratio of CH$_4$: CO$_2$: H$_2$: CO : N$_2$=1 : 1 : 2 : 0.3 : 0.3 and a GHSV of 500 L/h·g$_{cat}$. At the start of the reaction, CH$_4$ conversion for the 10Ni/MgAl$_2$O$_4$ and 10Ni-1K/MgAl$_2$O$_4$ catalysts was 44.8% and 59.4%, respectively. CH$_4$ conversion gradually decreased as the reactions proceeded, but the 10Ni-1K/MgAl$_2$O$_4$ catalyst exhibited higher and more stable activity as compared with that of the 10Ni/MgAl$_2$O$_4$ catalyst.

After the CO$_2$ reforming of COG, the used catalysts were observed by SEM for observing the formation of coke on their surfaces (Fig. 5). Notably, the 10Ni/MgAl$_2$O$_4$ catalyst exhibited large amounts of whisker coke, whereas the 10Ni-1K/MgAl$_2$O$_4$ catalyst did not exhibit any whisker coke. Fig. 6 shows the results obtained for TG analysis, which was performed for quantitatively analyzing the amount of coke deposited on the catalyst surface. TG curve exhibited sample weight loss with increasing temperature under air. Both samples exhibited an initial weight loss up to 350 ^{o}C, attributed to the oxidation of amorphous coke, which can be easily
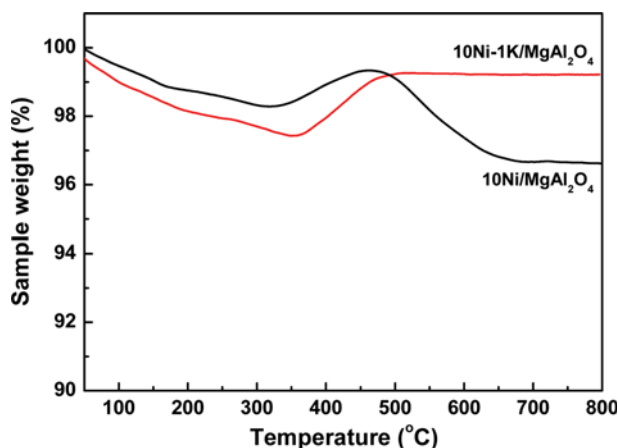
oxidized, and the thermal desorption of H$_2$O and CO$_2$ from the sample surface. Meanwhile, weight increase was observed in the 350-500 ^{o}C range, attributed to the oxidation of Ni exposed on the surface. Moreover, weight loss was also observed at temperatures greater than 500 ^{o}C, attributed to the gasification of graphite carbon to CO and CO$_2$ [13,18]. Between the 10Ni/MgAl$_2$O$_4$ and 10Ni-1K/MgAl$_2$O$_4$ catalysts, no significant decrease in terms of the sample weight was observed at temperatures less than 350 ^{o}C, corresponding to weight loss values of 1.6% and 2.4%, respectively. However, between the 10Ni/MgAl$_2$O$_4$ and 10Ni-1K/MgAl$_2$O$_4$ catalysts, significantly different weight loss values were observed at temperatures greater than 500 ^{o}C, attributed to the gasification of graphite carbon, corresponding to 2.7% and 0.1%, respectively. These results are in agreement with those obtained for SEM in Fig. 5. The 10Ni-1K/MgAl$_2$O$_4$ catalyst exhibited outstanding activity and coke resistance as the strong interaction between nickel and the support enhanced SMSI, and coke was easily removed, attributed to the improved coke gasification caused by the increased amount of adsorbed CO$_2$.

CONCLUSIONS

The promotion effects of K on the activity and coke resistance of a 10Ni/MgAl$_2$O$_4$ catalyst for the CSCR of COG were investigated. For the 10Ni-(x)K/MgAl$_2$O$_4$ catalyst, CO$_2$ adsorption increased because of the basicity of K. As compared to the 10Ni/MgAl$_2$O$_4$ catalyst, the 10Ni-(x)K/MgAl$_2$O$_4$ catalyst exhibited higher reduction temperature, attributed to the improvement of SMSI. The 10Ni-(x)K/MgAl$_2$O$_4$ catalyst exhibited activity higher than that of the 10Ni/MgAl$_2$O$_4$ catalyst for the CSCR of COG. Furthermore, the H$_2$/CO ratio of syngas was controlled by varying the feed ratio of H$_2$O and CO$_2$ in the CSCR of COG. The 10Ni-1K/MgAl$_2$O$_4$ catalyst with 1 wt% K exhibited outstanding activity and coke resistance; hence, the promotion of K results in the improvement of catalytic performance and the coke resistance of the 10Ni/MgAl$_2$O$_4$ catalyst for the CSCR of COG, attributed to the SMSI enhancement and CO$_2$ adsorption.

Fig. 6. TG profiles of used 10Ni/MgAl$_2$O$_4$ and 10Ni-1K/MgAl$_2$O$_4$ catalysts (Reaction conditions: CH$_4$: CO$_2$: H$_2$: CO : N$_2$=1 : 1 : 2 : 0.3 : 0.3, GHSV=500 L/h·g$_{cat}$, 800 ^{o}C, 5 atm, TOS=50 h).

REFERENCES

1. L. Xu, H. Song and L. Chou, *Int. J. Hydrogen Energy*, **38**, 7307 (2013).
2. W. H. Chen, M. R. Lin, A. B. Yu, S. W. Du and T. S. Leu, *Int. J. Hydrogen Energy*, **37**, 11748 (2012).
3. J. M. Bermudez, A. Arenillas, R. Luque and J. A. Menendez, *Fuel Process. Technol.*, **110**, 150 (2013).
4. Y. Zhang, J. Liu, W. Ding and X. Lu, *Fuel*, **90**, 324 (2011).
5. Z. Yang, W. Ding, Y. Zhang, X. Lu, Y. Zhang and P. Shen, *Int. J. Hydrogen Energy*, **35**, 6239 (2010).
6. J. Guo, Z. Hou, J. Gao and X. Zheng, *Energy Fuels*, **22**, 1444 (2008).
7. R. Razzaq, C. Li and S. Zhang, *Fuel*, **113**, 287 (2013).
8. B. Yue, X. Wang, X. Ai, J. Yang, L. Li, X. Lu and W. Ding, *Fuel Process. Technol.*, **91**, 1098 (2010).
9. J. E. Park, K. Y. Koo, U. H. Jung, J. H. Lee, H. S. Roh and W. L. Yoon, *Int. J. Hydrogen Energy*, **40**, 13909 (2015).
10. W. H. Chen, M. R. Lin, T. S. Leu and S. W. Du, *Int. J. Hydrogen Energy*, **36**, 11727 (2011).
11. Z. Yang, Y. Zhang, X. Wang, Y. Zhang, X. Lu and W. Ding, *Energy Fuels*, **24**, 785 (2010).
12. K. Y. Koo, J. H. Lee, U. H. Jung, S. H. Kim and W. L. Yoon, *Fuel*, **153**, 303 (2015).
13. K. Y. Koo, H. S. Roh, Y. T. Seo, D. J. Seo, W. L. Yoon and S. B. Park, *Appl. Catal. A: Gen.*, **340**, 183 (2008).
14. Y. H. Kim, K. Y. Koo and I. K. Song, *Korean Chem. Eng. Res.*, **47**(6), 700 (2009).
15. S.-H. Song, J.-H. Son, A. W. Budiman, M.-J. Choi, T.-S. Chang and C.-H. Shin, *Korean J. Chem. Eng.*, **31**(2), 224 (2014).
16. N. Majidian, N. Habibi and M. Rezaei, *Korean J. Chem. Eng.*, **31**(7), 1162 (2014).
17. K. I. Moon, C. H. Kim, J. S. Choi, S. H. Lee, Y. G. Kim and J. S. Lee, *Korean Chem. Eng. Res.*, **35**(6), 890 (1997).
18. K. Y. Koo, H. S. Roh, U. H. Jung, D. J. Seo, Y. S. Seo and W. L. Yoon, *Catal. Today*, **146**, 166 (2009).
19. F. Frusteri, F. Arena, G. Calogero, T. Torre and A. Parmaliana, *Catal. Commun.*, **2**, 49 (2001).
20. A. E. C. Luna and M. E. Iriarte, *Appl. Catal. A: Gen.*, **343**, 10 (2008).
21. J. J. Juan, M. C. R. Martínez and M. J. I. Gomez, *Appl. Catal. A: Gen.*, **301**, 9 (2006).
22. X. Hu and G. Lu, *Green Chem.*, **11**, 724 (2009).
23. X. Yu, S. Zhang, L. Wang, Q. Jiang, S. Li and Z. Tao, *Fuel*, **85**, 1708 (2006).
24. N. Iwasa, T. Yamane and M. Arai, *Int. J. Hydrogen Energy*, **36**, 5904 (2011).